Received: 23 September 2019 | Accepted: 5 July 2020

DOI: 10.1002/sctm.19-0315

TISSUE ENGINEERING AND REGENERATIVE MEDICINE

STEM CELLS TRANSLATIONAL MEDICINE

Injectable *BMP-2* gene-activated scaffold for the repair of cranial bone defect in mice

Kai Sun | Hang Lin | Ying Tang | Shiqi Xiang | Jingwen Xue | Weifeng Yin | Jian Tan | Hao Peng | Peter G. Alexander | Rocky S. Tuan | Bing Wang

Department of Orthopaedic Surgery, University of Pittsburgh School of Medicine, Pittsburgh, Pennsylvania

Correspondence
Bing Wang, MD, PhD, and Rocky S. Tuan, PhD, Department of Orthopaedic Surgery, University of Pittsburgh School of Medicine, 450 Technology Drive, Pittsburgh, PA 15219.
Email: bingwang@pitt.edu (B. W.) and rst13@pitt.edu (R. S. T.)

Present address
Kai Sun and Hao Peng, Department of Orthopaedics, Renmin Hospital of Wuhan University, Wuhan, People's Republic of China

Ying Tang, Center for Pulmonary Vascular Biology and Medicine, Department of Medicine, University of Pittsburgh School of Medicine, Pittsburgh, Pennsylvania

Shiqi Xiang, Department of Orthopaedics, Xiangya Hospital, Zhongnan University, Changsha, HunanPeople's Republic of China

Jingwen Xue, Department of Dermatology, Beijing Tsinghua Changgung Hospital, Tsinghua University, Beijing, People's Republic of China

Weifeng Yin, Department of Orthopaedics, Tongji Hospital, Huazhong University of Science and Technology, Wuhan, People's Republic of China

Rocky S. Tuan, Institute for Tissue Engineering and Regenerative Medicine, The Chinese University of Hong Kong, Hong Kong SAR, People's Republic of China

Funding information
Commonwealth of PA Department of Health, Grant/Award Numbers: SAP4100062224, SAP4100050913, SAP4100065563,

Abstract

Tissue engineering using adult human mesenchymal stem cells (MSCs) seeded within biomaterial scaffolds has shown the potential to enhance bone healing. Recently, we have developed an injectable, biodegradable methacrylated gelatin-based hydrogel, which was especially effective in producing scaffolds in situ and allowed the delivery of high viable stem cells and gene vehicles. The well-demonstrated benefits of recombinant adeno-associated viral (rAAV) vector, including long-term gene transfer efficiency and relative safety, combination of gene and cell therapies has been developed in both basic and translational research to support future bone tissue regeneration clinical trials. In this study, we have critically assessed the applicability of single-step visible light (VL) photocrosslinking fabrication of gelatin scaffold to deliver rAAV encoding *human bone morphogenetic protein-2* (*BMP-2*) gene to address the need for sustained BMP-2 presence localized within scaffolds for the repair of cranial bone defect in mouse model. In this method, rAAV-BMP-2 and human bone marrow-derived MSCs (hBMSCs) were simultaneously included into gelatin scaffolds during scaffold formation by VL illumination. We demonstrated that the subsequent release of rAAV-BMP-2 constructs from the scaffold matrix, which resulted in efficient in situ expression of *BMP-2* gene by hBMSCs seeded within the scaffolds, and thus induced their osteogenic differentiation without the supplement of exogenous BMP-2. The reparative capacity of this novel stem cell-seeded and gene-activated scaffolds was further confirmed in the cranial defect in the severe combined immunodeficiency mice, revealed by imaging, histology, and immunohistochemistry at 6 weeks after cranial defect treatment.

KEYWORDS

BMP-2 gene activated scaffold, bone formation, cranial defect, hBMSCs, rAAV

Kai Sun and Hang Lin contributed equally to this study.

SAP4100061184; National Institutes of Health, Grant/Award Number: 5R01EB019430; U.S. Department of Defense, Grant/Award Numbers: W81XWH-14-2-0003, W81XWH-10-1-0850

1 | INTRODUCTION

Bone is one of the most commonly repaired tissues of human beings; however, there were approximately 6.5 million patients with bone fractures who suffered from fracture-delayed unions or nonunions reported in the US yearly.[1] Bony defects in the craniomaxillofacial skeleton remain a major and challenging health concern.[2] Although autologous bone grafts have been considered as the clinical "gold standard" for bone defects,[3,4] this method is restricted by tissue availability and surgical complications, for example, donor site pain and morbidity.[5] The combinational uses of scaffolds, stem cells, and growth factors have shown its potential to promote bone defect repair. Adult mesenchymal stem cells (MSCs) seeded within biomaterial scaffolds have been successfully explored to enhance bone healing.[6,7] A major requirement in stem cell-based bone tissue engineering is to promote robust osteogenic differentiation of cells seeded within biomaterial scaffolds, which require the localized and sustained introduction of osteoinductive biofactors.[8] In order to enhance the efficiency of transduction of biofactors to stem cells, biomaterial-based therapeutic gene delivery has been used as an alternative to traditional ex vivo gene therapy that requires complicated cell culture and preparation time in vitro.[9,10] To fabricate gelatin scaffolds fitting local structural variation in different bones and defects, we recently developed a visible light (VL)-based projection stereolithographic fabrication of biodegradable osteoinductive gene-activated methacrylated gelatin (mGL) scaffold that is compatible with *human bone morphogenetic protein-2* (*BMP-2*) gene and human bone marrow-derived stem cells (hBMSCs) for bone tissue engineering.[11] In previous studies, viral vectors have been demonstrated to be an effective and safe *BMP-2* gene delivery vehicle through in vivo[12] and ex vivo[13] gene therapy. We used recombinant adeno-associated viral (rAAV) as the delivery vehicle to transduce human *BMP-2* gene into hBMSCs through a single step procedure that skips in vitro preparation time.[14] Expression of *BMP-2* gene was determined by enzyme-linked immunosorbent assay (ELISA) assay. The osteogenesis of the transduced hBMSCs was then assessed through real-time PCR. rAAV-vector-based local in situ gene transfer in overcoming the clinical limitations of BMP-2 protein delivery and a traditional ex vivo *BMP-2* gene transduction procedure. Here, we describe the design and preparation of one-step combination of gene and cell with VL photocrosslinking (VL-PXL) technology for the repair of cranial bone defects in mice. The goal of current proof-of-concept study is the assessment of the potential applicability of the VL-PXL-based scaffold preparation method for the production of biologically active gene-activated scaffold for hBMSC-based bone formation. in vivo bone formation efficacy was tested in a severe combined immunodeficiency (SCID) mouse model with a surgically created cranial bone defect. The new bone formation was estimated by micro-computed tomography (micro-CT), H&E staining, and osteocalcin immunohistochemistry (IHC). hBMSCs within the scaffolds showed high viability within gelatin scaffolds by VL-PXL technology. Like our previous studies,[11,14] sustained *BMP-2* gene expression and differentiated toward osteogenic lineage were observed and we did not find cytotoxicity in *BMP-2* gene transduced hBMSCs. The analyses from micro-CT image, new bone volume (BV), and bone mineral density (BMD) indicated bone formation of hBMSCs encapsulated in *BMP-2* gene-activated gelatin scaffold as early as 6 weeks postimplantation. The matured trabecular bone tissue formation was also revealed by H&E staining and IHC.

The results showed potential applications of a one-step VL-PXL fabrication method for biomaterial scaffold to enhance bone formation in local structural variation in different bones and defects model.

Significance statement

This article describes a novel and advanced method of providing recombinant adeno-associated viral (rAAV)-human bone morphogenetic protein-2 (BMP-2) to human bone marrow-derived mesenchymal stem cells, a promising source of cells for regenerative medicine, encapsulated in the visible light photocrosslinking (VL-PXL) technology fabricated gelatin scaffold. In particular, live-dead staining and rAAV release kinetics assay were performed, to estimate the safety and efficiency of the scaffold-based delivery system. The in vivo study further showed the capacity of this new system in repairing the bone defect. This novel gene-engineered, cell-based, VL-PXL fabricated bone construct thus represents a robust treatment method for the mouse cranial defect.

2 | MATERIALS AND METHODS

2.1 | Human sample collection and animal study

Human tissues for the isolation of hBMSCs were from the patient who underwent total hip arthroplasty with the approval from the Institutional Review Board approval (University of Washington and University of Pittsburgh) according to our published protocol[15] and all animal experiments and procedures were approved by the Institutional Animal Care and Use Committee of the University of Pittsburgh, under a protocol (17121844).

2.2 | hBMSCs isolation

The hBMSCs were isolated as previously described[11,14,16,17] and cultured in proliferation medium (PM) (GM; α-MEM +1%

Antibiotic-Antimycotic +10% fetal bovine serum [FBS]; Gibco/Life Technologies, Grand Island, New York) and 1 ng/mL Fibroblast Growth Factor 2 (FGF-2, R&D Systems, Minneapolis, Minnesota), the hBMSCs were then plated into T150 tissue culture flasks and cultured in 37°C with 5% CO_2. The nonadherent cells were washed by phosphate-buffered saline after 3 days culture, and GM were changed every 3 days. 0.25% trypsin containing 1 mM EDTA (Invitrogen, Carlsbad, California) were used to detach cells when reached 70% to 80% confluence, then passaged. Cells of passage 3 were used to perform this experiment.

2.3 | Gene delivery system

Human *BMP-2* and *green fluorescent protein* (*GFP*) genes were both carried by the double-stranded rAAV vectors[18] under the control of the human cytomegalovirus (CMV) immediate early enhancer and promoter, respectively. According to our published protocols,[19,20] serotypes 6 of rAAV vectors (BMP-2 and GFP) were packaged using an adeno-free, triple-plasmids co-transfection system in 293 cells. The vector preparations were purified by twice CsCl gradient ultracentrifugation and the final rAAV viral genome copies (v.g.) were measured by DNA dot blot[19] and were in the range of 5×10^{12} to 2×10^{13} v.g. particles/mL.

2.4 | rAAV6-GFP transduction efficiency in mGL hydrogel scaffold

As we described previously,[11] the mGL was dissolved into Hank's balanced salt solution (HBSS, Invitrogen) at 10% (w/v), 1 N NaOH was used to adjust the pH of solution to 7.4, and then, photoinitiator lithium phenyl-2, 4,6-trimethylbenzoyl phosphinate (LAP) was added into mGL solution at 0.15% (w/v). 1×10^6 of hBMSCs were mixed with 1, 5, 10, and 20 μL rAAV6-GFP (vectors titers was 1.0×10^{13} v.g. particles/mL), respectively, and suspended in 50 μL of mGL/LAP solution, there were multiplicity of infection (m.o.i.) of 1×10^4 rAAV/cell group, 5×10^4 rAAV/cell group, 1×10^5 rAAV/cell group and 2×10^5 rAAV/cell group. The mixed solution was poured into the 2-mm-height mold and a dental curing light (Mega Light CL; DBI America, Lutz, Florida), producing VL at 430-490 nm wavelength and 1400 mw/cm^2 power, and then was applied to directly irradiate the mGL/LAP solution for 4 minutes. The photopolymerized mGL hydrogel was punched into 5-mm-diameter by 2-mm-height cylinders. The seeded mGL hydrogel cultured in DMEM without FBS overnight. After that, 1 mL of complete medium (DMEM+ 1× Antibiotic-Antimycotic +10% FBS; all Gibco/Life Technologies) was added on day 2. After day 4, the transduced hBMSCs were identified under the fluorescence microscope and we counted the rAAV6-GFP infection efficiency (positive green cells/total cells).

2.5 | Comparing the transduction efficiency in hBMSCs between 3D and 2D culture

The functionality of injectable gene-activated scaffold for the repair of cranial bone defect depends on the efficiency of gene transduction of seeded hBMSCs in 3D condition. According to our previous studies that we detected gene transduction efficiency within 3D environment,[11,14] here, we compared the GFP expression level in 3D culture within hydrogel and 2D culture using the same density of hBMSCs with infection at a low level of m.o.i. of rAAV6-GFP (1×10^4 rAAV/cell) on day 4.

2.6 | Bone scaffold fabrication using VL-PXL fabrication technology

We have used photocrosslinkable mGL as the starting material for scaffold fabrication. Photocrosslinking was mediated with the photoinitiator, LAP. The necessary reagents and procedures have been used in our previous publications.[10] mGL was prepared as described previously.[15] Briefly, 3% aqueous gelatin solution was reacted with methacrylic anhydride for 16 hours, dialyzed extensively against H_2O to remove unreacted reagents, lyophilized, and kept in dark until use. LAP, serving as VL-activated photoinitiator, had an absorbance ranging from ultraviolet (210 nm) to visible (500 nm) light. It was synthesized by reacting dimethyl phenylphosphonite (Acros Organics, New Jersey) with 2,4,6-trimethylbenzoyl chloride via a Michaelis-Arbuzov reaction.[21] In details, the mGL was dissolved into HBSS (Invitrogen) at 10% (w/v), 1 N NaOH was used to adjust pH of solution to 7.4, and then, photoinitiator LAP was added into mGL solution at 0.15% (w/v). 1×10^{12} v.g. particles of rAAV6-BMP-2 and 1×10^7 hBMSCs were mixed into 500 μL of mGL/LAP solution. The mixed solution was poured into the 2-mm-height mold and a dental curing light (Mega Light CL; DBI America), producing VL at 430 to 490 nm wavelength and 1400 mw/cm^2 power, was applied to directly irradiate the mGL/LAP solution for 4 minutes. The photopolymerized mGL hydrogel was punched into 5-mm-diameter by 2-mm-height cylinders. The mGL hydrogel was cultured in complete medium (DMEM+ 1× Antibiotic-Antimycotic +10% FBS) containing hBMSCs and rAAV6-BMP-2, this was named "One step group." The "Control group" used the same condition to encapsulate naïve hBMSCs to construct photopolymerized mGL hydrogel. The "Protein group" encapsulated naïve hBMSCs using the same condition but included 50 ng/mL BMP-2 (final concentration).[22] rAAV6-BMP-2 ex vivo gene transfer to hBMSCs, prior to their seeding onto biomaterial scaffolds, were fabricated using the same conditions and named "Ex vivo group." The medium of "Control group" and "One step group" were changed at day 1, day 2, day 4, and then every 3 days using complete medium (DMEM+ 1× Antibiotic-Antimycotic +10% FBS) until day 28. The medium of "Protein group" and "Ex vivo group" were changed at day 2, day 4, and then every 3 days using complete medium (DMEM+ 1× Antibiotic-Antimycotic +10% FBS) until day 28.

2.7 | Protein and gene expression analyses

To confirm in vitro functionality of rAAV6-BMP-2 construct, the supernatant of the hBMSC-seeded, gene-activated constructs cultured from day 1 to day 14 was processed for BMP-2 protein ELISA assay. Four groups, including (a) Control group, (b) Protein group, (c) One step group, and (d) ex vivo group, were carried out according to the manufacturer's protocol (R&D Systems). Gene expression in the constructs after 28 days of culture was also carried out using RNA extracted from the samples using

an RNeasy plus mini kit (QIAGEN Sciences, Valencia, California). Reverse transcription-PCR (RT-PCR) was performed using SYBR Green PCR master mix (Applied Biosystems, Foster City, California) on a 7900HT Fast Real-Time PCR machine (Applied Biosystems) or StepOnePlus thermocycler (Applied Biosystems) under the following conditions at 94°C for 5 minutes, 40 cycles of 94°C for 30 seconds, 60°C for 30 seconds, 72°C for 30 seconds, and 72°C for 5 minutes. Transcription level of GADPH was used as endogenous control: forward, 5′-AA TCCCATCACCATCTTCCA-3′ and reverse, 5′-TGGACTCCACGACGTAC TCA-3′. The primer sequences for osteocalcin (OCN) and alkaline phosphatase (ALP) were as follows: forward, 5′-TGACGAGTTGGCTGACCA-3′ and reverse, 5′-AGGGTGCCTGGAGAGGAG-3′; forward, 5′-GACC TCCTCGGAAGACACTC-3′ and reverse, 5′-TGAAGGGCTTCTTGTCTG TG-3′, respectively. The results were analyzed using the comparative CT method according to our published protocol.[14]

2.8 | rAAV particle release kinetics

Based on high efficiency of serotype 6 of rAAV vector in hBMSCs,[14] it was selected for all subsequent in vitro and in vivo experiments. Because controlled release of viral particles from the gene-activated VL-PXL fabricated 3D gelatin scaffold is critical to the success of gene transduction of the seeded hBMSCs, dot blot assay was performed to assess the kinetics of viral release from the mGL scaffold. rAAV gene-activated scaffolds prepared using the fabrication method described above were ethanol-sterilized, rinsed in DMEM, and then incubated in 100 μL of DMEM. An aliquot of the incubating medium was collected at different time points lasting for 28 days. Dot blot assay was used to quantify the v.g. copy number in the daily aliquot of conditioned medium and assess release kinetics of viral vector from the gene-activated hydrogel scaffold. The results were analyzed for the release of viral particles from the scaffold with a dot blot hybridization assay using a CMV promoter probe.[14] Since we used double-strand rAAV, the number of virus particles is half the number of virus genomes. The "One step" group medium contained the released viral particles from the scaffold was used to detect the number of rAAV vector particles released from mGL hydrogel.[19,23]

2.9 | Creation of mouse critical-sized cranial bone defects

Male SCID mice (8-12 weeks old; NOD.CB17PRKDA SCID/J, Jackson Laboratory, Bar Harbor, Maine) were performed in this experiment to create cranial bone defects according to published protocols.[24,25] Prior to surgery, the mice were anesthetized with 4% isoflurane for induction. A state-of-the-art gas delivery and scavenging system was in place to capture the isoflurane, which was validated by the supplier. A maintenance schedule was also in place. After hair was shaved and disinfectant was applied, the surgical site was then be surrounded by a sterile drape, and a 1 cm skin incision was then made along the midline of the skull. As shown in Figure 1, a 5-mm diameter bone defect was made by trephine (18004-50; Fine Science Tools, Foster City, California). The bone was carefully removed, and the defect area was rinsed with normal saline. The mGL hydrogel scaffold of the same size filled the cranial defect (depth of gel = 1 mm), and then the wound was closed with 5-0 nylon suture. Compositional requirement was assessed by comparison between various combinations that include four conditions (six mice per condition, according to power analysis for significance, for a total of 24). The four groups were: (a) mGL hydrogel loaded with hBMSCs (Control group); (b) mGL hydrogel loaded with BMP-2 protein (50 ng/mL) and hBMSCs (Protein group); (c) mGL hydrogel loaded with rAAV6-BMP-2 and hBMSCs (One step group); and (d) mGL hydrogel loaded with hBMSCs that were prior transduced ex vivo with rAAV6-BMP-2 (Ex vivo group).

2.10 | In vivo bone regeneration

To visualize and quantify bone formation, treated mice were anesthetized and micro-CT scans (Viva CT-40, ScancoMedical, Switzerland) was used to scan the skull bone to evaluate the bone healing process using a 30-μm voxel size and medium resolution, including analysis of BV and density at 6 weeks. 3D reconstructions were created after obtaining 2D image slices from the micro-CT. BV and BMD were quantified using Scanco evaluation software according to the guidelines of the American Society of Bone and Mineral Research.

2.11 | Histology

At 6 weeks after cranial defect treatment, the samples were collected for hematoxylin and eosin (H&E) staining. The samples were fixed by 10% formalin for 24 hours. After that, 10% EDTA-2Na+ 1% NaOH were utilized to decalcify for 24 hours, and then were embedded in paraffin and sectioned (8 μm thicknesses). Samples were also collected for immunohistochemical (IHC) stainings to analyses the expression of the *OCN* gene. Briefly, sodium citrate buffer was used to retrieve antigen for 20 minutes at 95°C, nonspecific binding was suppressed with for 1 hour at room temperature. Samples were incubated with rabbit anti-OCN primary antibody (1:200) (Abcam ab93876, Cambridge, Massachusetts) overnight at 4°C, then incubated with horse anti-rabbit biotinylated secondary antibodies (Vector Laboratories, Burlingame, California) 30 minutes. Samples were incubated with horseradish peroxidase-conjugated streptavidin (Vector Laboratories) and treated with the Vector NovaRED peroxidase substrate (Vector Laboratories). After IHC, samples were then subsequently counterstained with hematoxylin, dehydrated, mounted, cover slipped. The images were captured by the Olympus CKX41 microscope.

2.12 | Statistical analysis

Data are presented as mean ± SD. Statistical significance between two groups was evaluated by two-tailed Student's *t* test. ANOVA followed by post hoc analysis for multiple-group comparisons. $P < .05$ were considered significant. All of in vitro experimental were performed triple samples in each group.

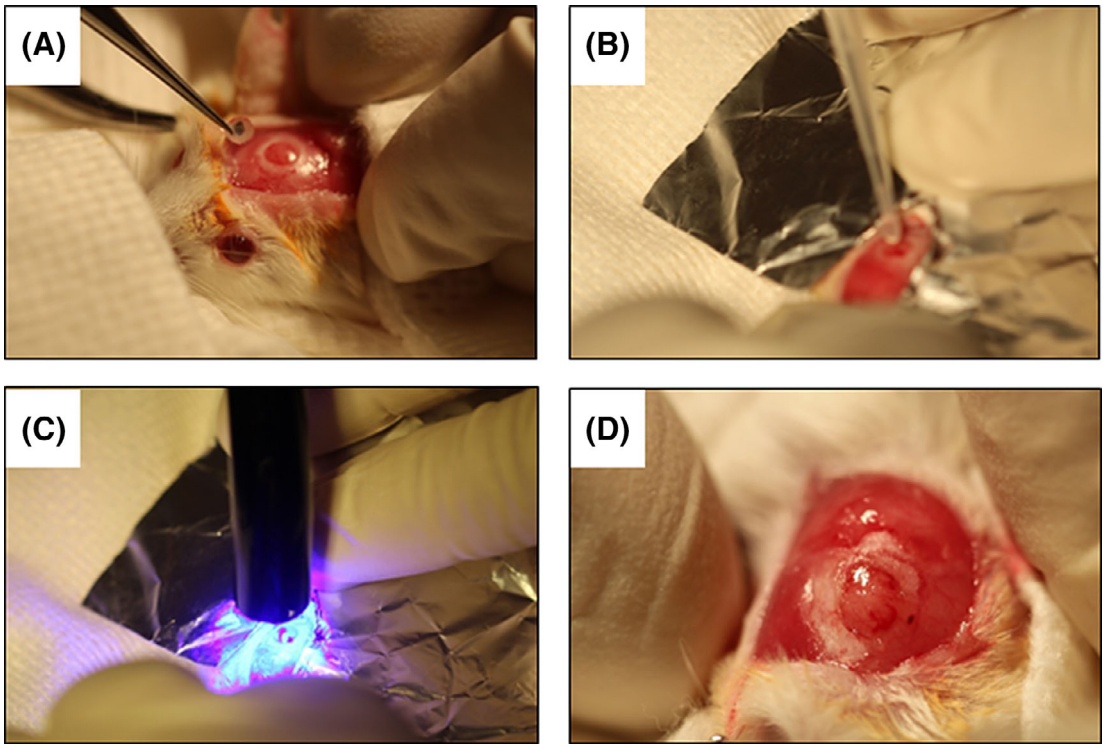

FIGURE 1 After hair was shaved and disinfectant was applied, a 1 cm skin incision was made along the midline of the skull. A 5-mm diameter bone defect was created by trephine (A). Methacrylated gelatin (mGL) hydrogel scaffold containing recombinant adeno-associated viral (rAAV)-human bone morphogenetic protein-2 (BMP-2) and human bone marrow-derived mesenchymal stem cells (hBMSCs) was able to fill the cranial defect and maintain the position (B). Using visible light photocrosslinking (VL-PXL) technology, hydrogel was cross-linked (C) and stabilized (D) that allows mGL hydrogel scaffold to fill the cranial defect. Skin was then closed with suture

3 | RESULTS

3.1 | Efficiency of gene expression in hBMSCs within hydrogel scaffold

The transduction efficiency of *BMP-2* gene within the scaffolds was assessed by the expression of *GFP* gene. rAAV6-GFP virus was chosen for investigation of gene vector activity within scaffold instead of rAAV6-BMP-2 because that the GFP with green fluorescence was able to be visualized under immunofluorescence (IF) microscopy, allowing the calculating of GFP transduction efficiency. Since rAAV6-BMP-2 construct has the exact same rAAV backbone, both rAAV constructs (GFP and BMP-2) should have the same infection mechanism, when the same m.o.i. for hBMSC transduction is used. Before implantation of gene-activated scaffold, gene transfer efficiency within the mGL was assessed after 2 days on the basis of GFP fluorescence to confirm the rAAV dose using in modifying hBMSCs. Microscopic fields obtained by green fluorescence and phase contrast imaging were merged to determine infection efficiency. The GFP expression at the m.o.i. of 1×10^5 v.g. particles/cell group and 2×10^5 v.g. particles/cell group had significantly higher infection levels (*$P < .05$) comparing with the m.o.i. of 1×10^4 v.g. particles/cell group and 5×10^4 v.g. particles/cell groups in 3D environment (Figure S1A). We did not find significant difference ($P > .05$) between GFP expression in the m.o.i. of 1×10^5 v.g. particles/cell group and 2×10^5 v.g. particles/cell group, ranged from 45% to 50% (Figure S1B). The quantitative analysis indicated that the cell proliferative ratio at 1×10^5 v.g. particles/cell group had no negative effect on cell proliferation as compared to 2×10^5 v.g. particles/cell group (Figure S1C). As a proof of concept that allows usage of minimal doses, thereby avoiding toxicity while retaining high efficiency of gene transfer, we used the m.o.i. of 1×10^5 v.g. particles/cell for in the following experiments because this dose achieved a high level of gene expression in hBMSCs within scaffold.

3.2 | AAV vector release kinetics

According to previous experiments,[14] we have selected rAAV6 virus for all subsequent in vitro and in vivo experiments, and performed the Dot blot assay to detect the viral release kinetics from the mGL scaffold. We determined the release kinetics of rAAV6-BMP-2 released viral particles into the culture medium for up to 28 days. Dot blot assay was used to quantify the v.g. in the daily aliquot of conditioned medium and assess release kinetics of viral vector from the gene-activated scaffold. As shown in Figure 2A, the number of rAAV particles released daily reached peak value at day 16, reaching 4.8×10^9 v.g. particles/scaffold, and was substantially reduced starting at day 25. Finally, the release of only 2×10^9 v.g. particles was observed at day 28. The percentage of encapsulated rAAV particles released into the medium was less than 25% during 28 days culture, as demonstrated

in Figure 2B. The results demonstrated that mGL hydrogel had the ability of slowly releasing rAAV particles, indicating an extended effect of the mGL in delivering gene vectors, in addition to its function as a bioscaffold.

3.3 | *BMP-2* gene expression and osteogenic differentiation in hBMSCs

To determine the functionality of gene-activated hydrogel, the expression level of the transduced *BMP-2* gene in hBMSCs within the 3D constructs was then analyzed. Transduced cell laden scaffolds were cultured in basal growth medium, and then the BMP-2 concentration in the medium was measured by ELISA. Four groups were studied, which included: (a) mGL hydrogel loaded with hBMSCs (Control group); (b) mGL hydrogel loaded with BMP-2 protein (50 ng/mL BMP-2 [final concentration]) and hBMSCs (Protein group); (c) mGL hydrogel loaded with rAAV6-BMP-2 and hBMSCs (One step group); and (d) mGL hydrogel loaded with hBMSCs that were prior infected ex vivo with rAAV6-BMP-2 (Ex vivo group). The results showed that the *BMP-2* gene was efficiently expressed in the One step group, and reach the peak value at day 4, ranged from 1.0 to 1.5 ng/mL, which was closed to the range of BMP-2 concentrations (~10 ng/mL) often used to induce BMSCs osteogenesis in vitro.[26,27] Interestingly, the One step group had significantly higher BMP-2 expression levels (*P < .01) compared to other groups in days 2 and 4 (Figure 3).

We next assessed the extent of osteogenesis in the hBMSC cultures by means of qRT-PCR analysis of the OCN and the ALP after culture for 28 days. As shown in Figure 4A, the One step group has significantly higher *OCN* gene expression levels (**P < .01) compared to the other three groups. Moreover, the ALP was found at significantly higher levels (*P < .05) in the One step group and the Ex vivo groups comparing with Control group and Protein group, however, there were no significant difference (P > .05) between the One step group and the Ex vivo group (Figure 4B).

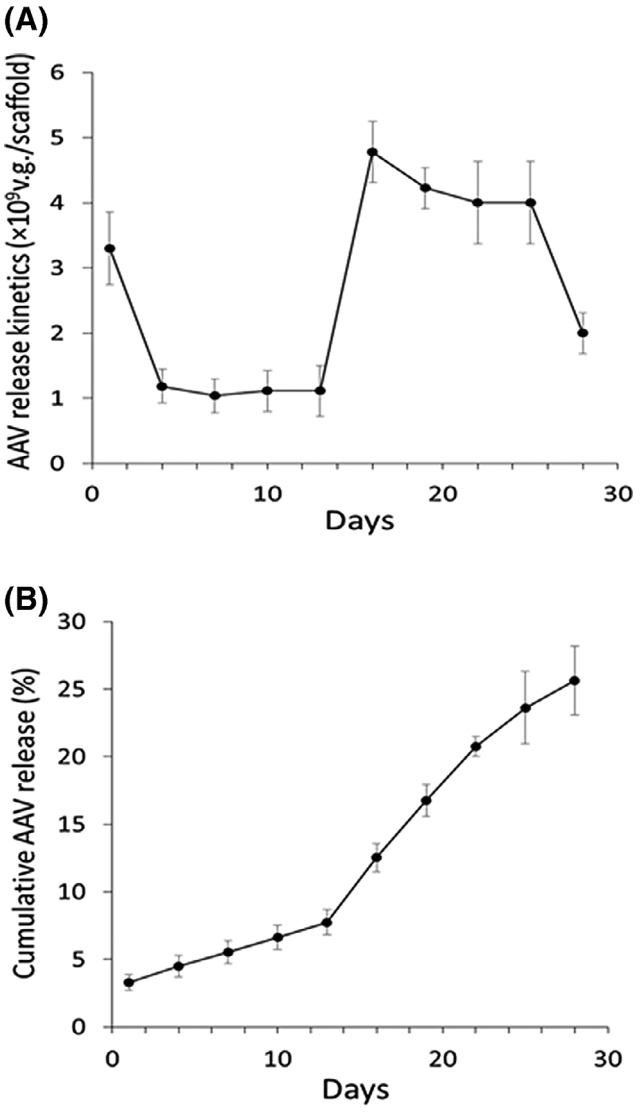

FIGURE 2 Release kinetics of adeno-associated viral (AAV) particles from Gene-Activated visible light photocrosslinking (VL-PXL) scaffold. A, Dot blot quantification of daily release of AAV-human bone morphogenetic protein-2 (BMP-2) v.g. of particles in incubation medium up to 28 days (initial load = 1.0×10^{12} v.g. particles/mL in 500 μL methacrylated gelatin [mGL] scaffold). B, The cumulative release over time clearly indicated a slow and minor release of AAV from hydrogel at the beginning (up to 14 days), and then a fast and major release from day 16. n = 3

3.4 | Micro-CT analyses

In order to test the reparative capacity of *BMP-2* gene activated VL-PXL scaffold, four groups (shown above) were examined by implanting mGL hydrogel constructs into cranial bone defect model of SCID mice. Micro-CT was used to scan the skull bone to evaluate the bone healing process at 6 weeks. Comparing with Control group and Protein group

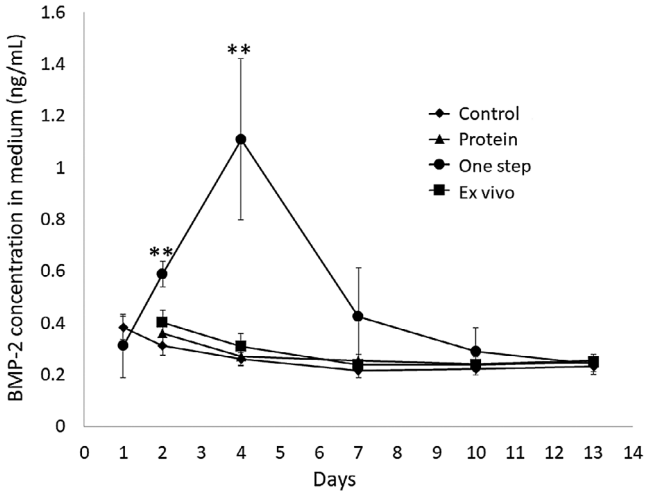

FIGURE 3 Human bone morphogenetic protein-2 (BMP-2) concentration (ng/mL) in the medium from four groups (Control, Protein, One step, and Ex vivo), which were determined for 1 to 14 days of culture by enzyme-linked immunosorbent assay (ELISA)

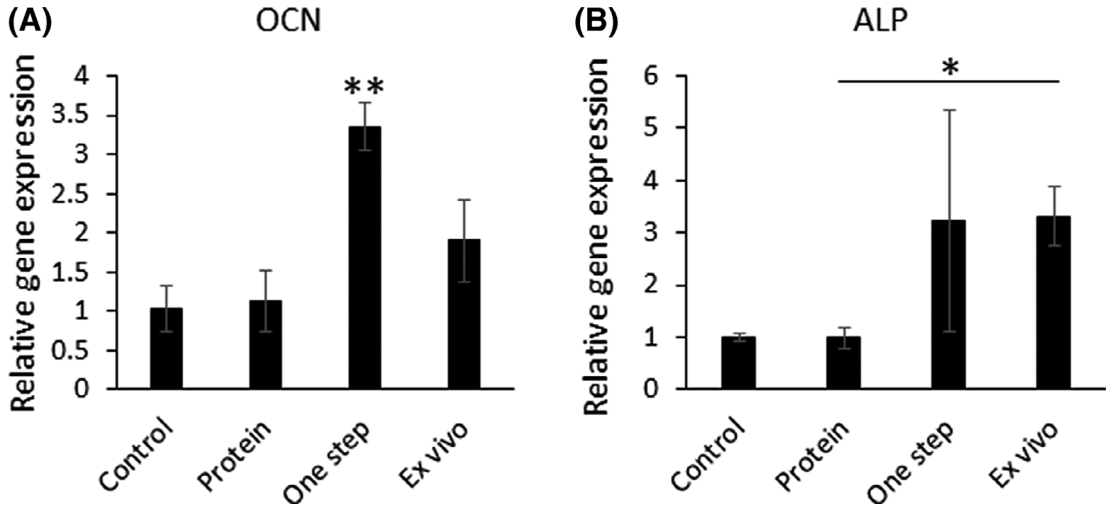

FIGURE 4 Examination of osteogenic gene expression using real-time PCR after culture for 28 days. The One step group had significantly a higher level of osteocalcin (*OCN*) gene expression compared to other three groups (A). The alkaline phosphatase (ALP) was found at significantly higher levels in One step group and ex vivo group compare to the Control group and Protein group (B)

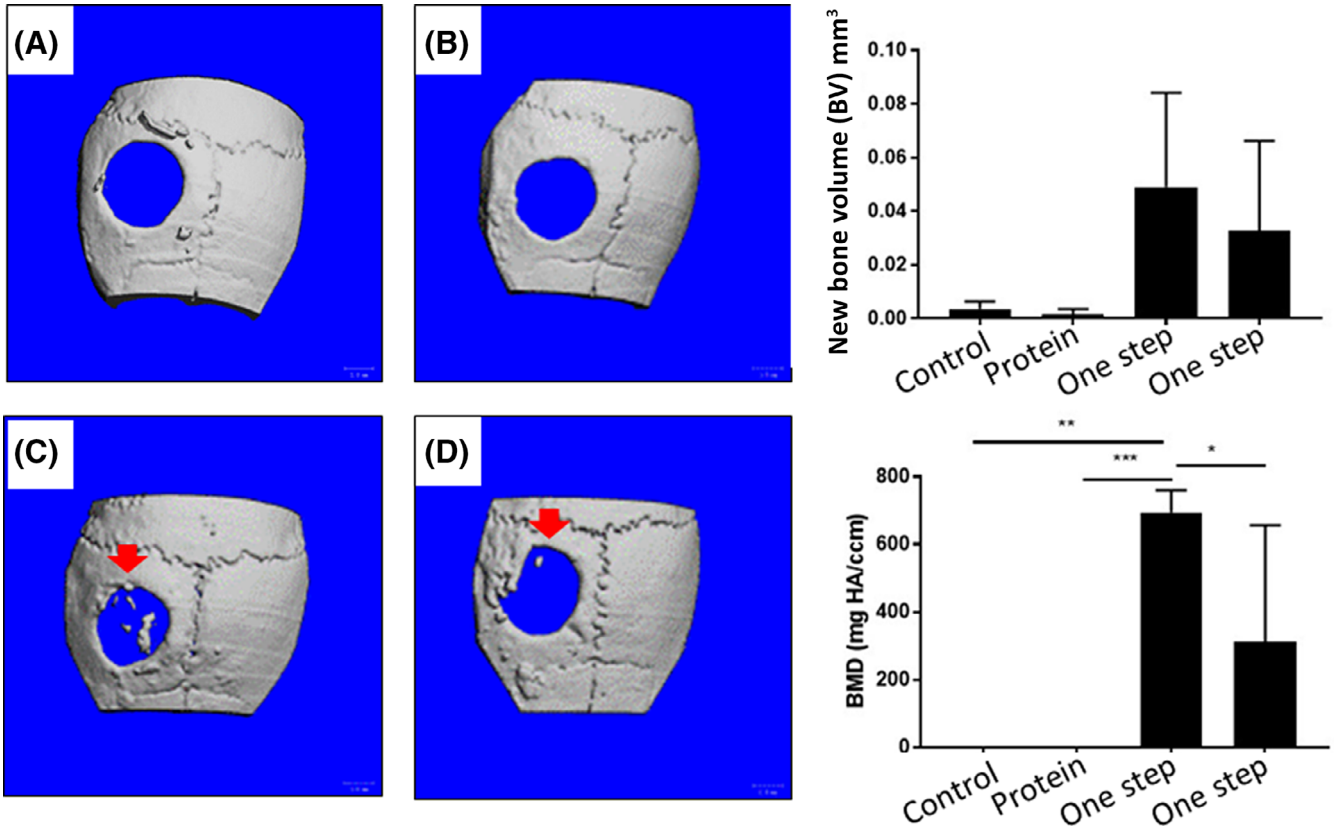

FIGURE 5 Micro-computed tomography (micro-CT) examination of bone formation in the animal study. No bone formation was observed in the implant site in the Control group and the Protein group after 6 weeks (A,B). New bony tissue (Red arrow) was formed in the cranium of the One step group and the ex vivo group (C,D). Quantitative analyses were performed on the bone volume (BV) and bone mineral density (BMD) values (n = 6, per group). **P* < .05; ***P* < .01, ****P* < .001

that no bone formation was observed in the defect site (Figure 5A,B), the One step group (mGL hydrogel loaded with rAAV6-BMP-2 and hBMSC) and Ex vivo group (mGL hydrogel loaded with rAAV6-BMP-2 transduced hBMSC) were capable of forming new bone in the calvarial bone defect site, as shown by 3D reconstruction of the micro-CT scans (Figure 5C,D). Quantitative analyses of BV and BMD (n = 6, per group) showed that there was no difference in new BV between the One step and the Ex vivo groups at 6-weeks post-treatment; however, the BMD in the One step group had the highest level as compared to the other three groups (*P < .05; **P < .01; ***P < .005).

3.5 | Histology

As shown in Figure 6A,B, the Control group and the Protein group were only showed fibrous tissues, and no bony tissue were observed. In the One step and the Ex vivo groups, new bone formation was observed in the area that was closed to native bone tissue (Figure 6C,D). Interestingly, the undegraded mGL hydrogel was observed in the One step group and the Ex vivo group as a result of excessive mGL hydrogel that was implanted into the cranial bone defect area, leading to meronecrobiosis.

We further performed the IHC to analyze the newly formed bone in the critical-sized calvarial bone defect model, as demonstrated by osteoinductive protein OCN staining. In the Control group, there were only a few of OCN positive area at the edge of bone defect area (Figure 7A, red arrow). We observed OCN positive area but no continuously bony tissue in the Protein group (Figure 7B, red arrow). As expected, new bone formation and OCN positive area were observed in both One step group and ex vivo group, over a wide area from the edges to the center of constructs (Figure 7C,D, red arrows), in which the osteocytes were massively noted in the interior of neo-bone.

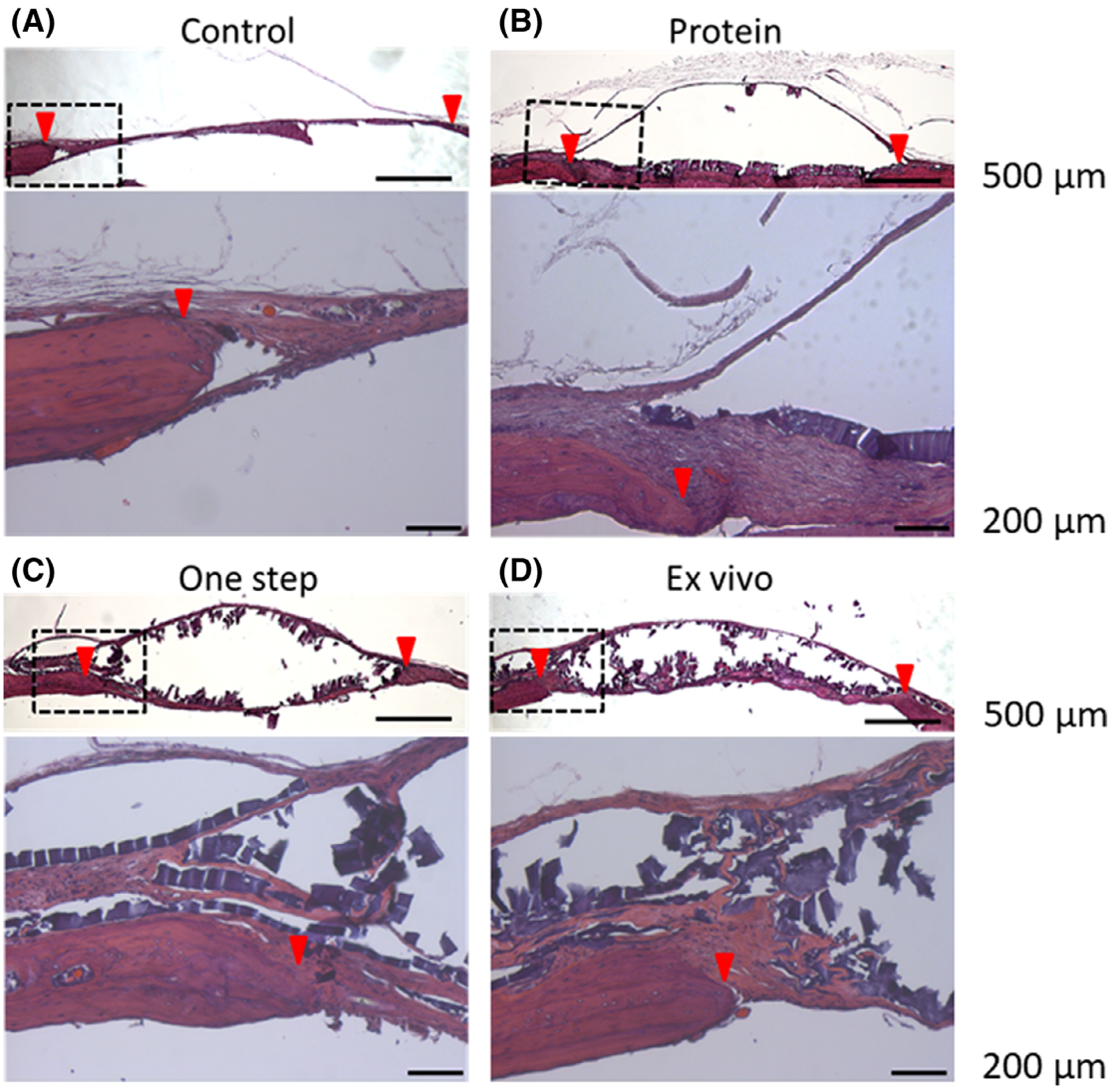

FIGURE 6 H&E analysis of samples from in vivo study. In the Control group and the Protein group, only fibroid tissues were observed without bony tissue (A,B). New bone formation and undegraded methacrylated gelatin (mGL) hydrogel constructs were observed in the One step group and the ex vivo group (C,D)

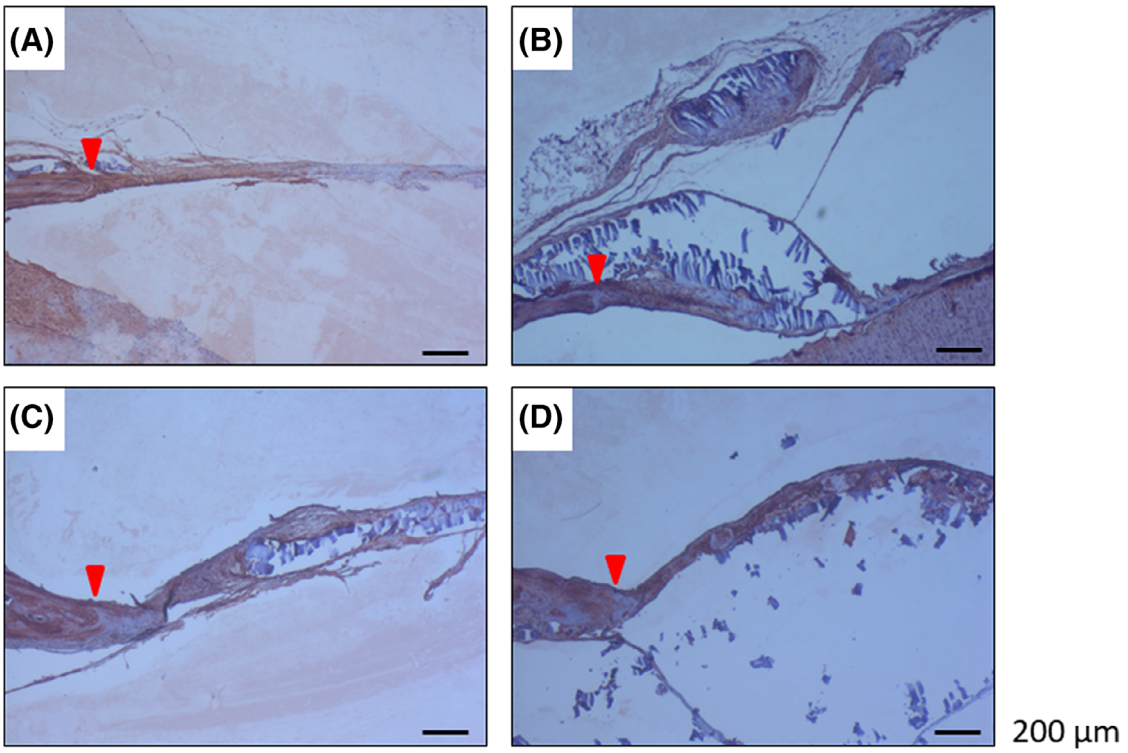

FIGURE 7 Assessment of bone formation with osteocalcin (OCN) immunohistochemistry (IHC). In the Control group, there were only a few of OCN positive area at the edge of bone defect area (A). In the Protein group, observe OCN positive area was observed but no continuously bony tissue (B). In the One step group and the ex vivo group (C,D), new bone formation and OCN positive area were observed over a wide area from the edges to the center of constructs

4 | DISCUSSION

In current study, we performed a parallel comparison of the capacity of an injectable, biodegradable mGL created by VL-PXL technology to repair the cranial bone defect in SCID mice. Four different constructs were incorporated with (a) naïve hBMSCs; (b) hBMSCs and BMP-2 protein; (c) hBMSCs and *BMP-2* gene vector; and (d) *BMP-2* gene transduced hBMSCs, respectively. The goal of this work was to engineer a hydrogel system for temporally controlled *BMP-2* gene vector delivery to encapsulated and surrounding cells for repair of full-thickness mouse cranial bone defect.

Cell-based bone tissue engineering involves the combination of cells, biomaterial scaffolds, and signaling molecules to restore, maintain or enhance bone tissue functions. Although significant progress in this area has been made in recent years, some key challenges, such as inadequate microenvironmental regulation of cell attachment, and proliferation and osteogenic differentiation within 3D biomaterial scaffolds, still remain. Most approaches used in previous studies, which involves the incorporation of soluble BMP-2 protein into the biomaterial scaffold[28] or using ex vivo gene transfer[10] to stem cells prior to their seeding onto scaffolds, have limited utility owing to BMP-2 short functional half-lives and rapid clearance by the bloodstream and time-consuming and cost-prohibitive additional cell-culture steps. There is therefore a critical need for the development of an effective gene delivery system to efficiently deliver growth factors, achieving sustained, long-term effect on stem cells seeded within the scaffold.

In view of the benefits of rAAV vectors, including long-term gene transfer efficiency and relative safety, combination of AAV-based gene and cell therapies are being developed in both basic and translational research, as well as in clinical trials for bone tissue regeneration. However, rAAV-based traditional ex vivo gene transfer to stem cells, prior to their seeding onto biomaterial scaffolds for tissue engineering and implantation, is still a time consuming process and requires complicated cell culture in vitro, which may change cell phenotype or function and increase infection risk.

To date, many investigators are highlighting the new trends in gene therapy research and clinical trials using matrix-based in situ gene transduction for bone tissue regeneration to avoid ex vivo transduction process.[29] So far, plasmid DNAs have reported successes in matrix-based gene delivery for tissue repair, but their use as a sole agent has been limited by rapid degradation and low gene transfer efficiency.[30] New trends in gene and cell therapy and clinical trials have highlighted the use of rAAV vectors for bone tissue regeneration over matrix-based plasmid DNAs delivery that is limited by rapid degradation and low gene transfer efficiency. The benefits of rAAV include high infection efficiency and lack of pathogenicity, thus eliminating the risk associated with persistent production of osteogenic factors. Recently, we developed one-step fabrication of rAAV-mediated *BMP-2* gene-activated porous poly-L-lactide scaffold for in vivo bone induction.[14] These findings strongly suggest that the combination of AAV-based gene transfer with biomaterials as a new paradigm for bone tissue engineering is efficient.

In current study, we have chosen gelatin hydrogel, fabricated by VL-PXL, as the biomaterial because of its biocompatibility and osteoconductive capacity.[31,32] It is not only biodegradable, therefore allowing tissue remodeling for new bone formation, but also hydrogel scaffold with nano-pores is desired to reduce free diffusion of rAAV gene vector comparing with other scaffolds with larger pores,[33,34] resulting in a safe localized osteogenic effect on hBMSCs. With mGL, we developed a VL-based photocrosslinking technology, using LAP photoinitiator and a dental light source, to prepare a highly reproducible 3D hydrogel scaffold. The resultant scaffold material is injectable and has good biodegradability and biocompatibility. As a hydrogel, it has good morphological form-fitting ability for different types of bone defect. VL initiated gelation takes place rapidly in air or aqueous solution after without the need for a protective barrier. The scaffold does not swell or contract during the process of osteoblast differentiation, and the integrity of the overall morphology is maintained. Moreover, the gelatin-based scaffold presents a highly conducive platform for the efficient transduction of hBMSCs with rAAV-BMP-2, as described in our previous studies of the bone formation model in the skeletal muscle of SCID mice.[10,11] Unlike *BMP-2* gene-activated porous poly-L-lactide scaffold for bone induction,[14] a major disadvantage of injectable gelatin is its low mechanical strength (~30 kPa compressive modulus), although a robust osteogenesis was observed in cranial bone defect model. In this study, gelatin was not expected to bear the mechanical load immediately. Given the biodegradation of gelatin and robust osteogenesis observed within the scaffold (Figures 6 and 7), rapid remolding and the formation of new bone should ensue, resulting in appropriate mechanical strength.

In term of the infection efficiency of rAAV gene vector into hBMSCs, results from different research groups are highly variable, which has a range from 8% to 52%,[35-37] depending on the serotype of rAAV, cell isolation protocol and the m.o.i. used. In current study, we achieved a gene transfer efficiency of 45% to 50% at m.o.i. of 1×10^5 v.g. in hydrogel 3D culture. Interestingly, we found that gelatin culture indicated a higher transduction efficiency than traditional tissue culture plastic (TCP) culture (Figure S2) at a low m.o.i. level (1×10^4 v.g.), suggesting the potential application of 3D hydrogel culture in enhancing the infection efficiency. The possible reason is the relative higher density of rAAV in gelatin culture. For example, under TCP culture, rAAV vectors were typically diluted into 20 mL culture medium, while in gelatin culture, same amount of AAVs were encapsulated into 50 to 200 μL of hydrogel. Consequently, there were more rAAV particles intensively surrounding the cells in such 3D culture condition. In fact, similar result was also reported. For example, the application of self-assembled poly(ethylene oxide) and poly(propylene oxide) triblock copolymers resulted in a more than 2-folder increase of infection efficiency, comparing to traditional methods.[38] Therefore, 3D culture condition may represent a more robust method to infect MSCs with rAAV vectors.

For effective application of gene-activated matrices for bone formation, it is important to control the amount and location of the expressed BMP-2 gene product in the newly formed bone. It has been shown[39] that gelatin has a natural capacity to bind viral particles, resulting in their slow release and higher infection efficiency in vivo; however, actual rAAV release kinetics in vivo was not reported in this literature. In our earlier study,[11] we investigated the controlled release of viral vectors from the scaffold used for bone formation, and concluded that a hydrogel scaffold with nano-sized pores is desirable to reduce free diffusion, compared to scaffolds with larger pores. In current study, we have also chosen gelatin hydrogel, fabricated by VL-PSL, as the biomaterial because of its biocompatibility and osteoconductive capacity. To assess the release kinetics of viral construct from the gene-activated mGL scaffold, dot blot assay was used to quantify viral genome copy number (v.g.) in a daily aliquot of conditioned medium. Compared to a PLLA scaffold, where fast release kinetics of rAAV particles was observed with two release peaks (day 5 and days 13-16),[14] the results of this study in Figure 2A showed a peak of daily release of 4.8×10^9 v.g. particles/scaffold starting on days 16 to 25. These results indicated a significantly slower kinetics of release of rAAV particles from the gelatin hydrogel compared to PLLA, and hence higher retention of rAAV particles within the gelatin hydrogel scaffold. In current study, rAAV particles were released from gelatin in a controlled manner, showing rAAV release robust increase from days 13 to 16 that is associated with gelatin biological characters such as degradation time point. As we tested the cultured hydrogel scaffold for days 1 to 14, the concentration of BMP-2 in the medium tested by ELISA assay was low in all four groups, including the Protein Group that we initially loaded 1 μg/mL of recombinant BMP-2. In comparison, another peptide-based hydrogel released most of AAVs in first 3 days.[40] In the same study, it also indicated the benefit of slow release of AAVs in enhancing the infection efficacy. After 28 days, there were around 28% vectors that were released. Therefore, 72% loaded AAVs were trapped in hydrogel, which dues to the slow in vitro degradation of photocrosslinkable gelatin. The density of gelatin may also play a critical role. For example, significantly less AAVs were released from fibrin in 7 days (from 95% down to 30%), when the concentration of fibrin increased from 10 to 50 mg/mL.[41] In fact, the high retention of AAVs within the scaffolds is desired for tissue engineering purpose, since we preferred to have AAVs only infect the cells locally within the scaffolds. The over release of AAVs may cause out-of-scaffold infection and osteogenesis, which might lead to the unwanted overgrowth of bone outside of defect area.

To examine the reparative capacity of single step-fabricated bone scaffolds in vivo, they were implanted into the cranial defect in SCID mice. In vivo murine systems, such as immunodeficient mice, have often been used to investigate the bone formation capacity of human bone fragment and human stem cell implantation in skeletal muscle, as well as bone repair in calvarial defect model in previous studies by us and others.[24,25,42,43] For human cell-based constructs for calvarial bone defect repair, SCID mice are also the suitable model due to low cost and ease in monitoring.[44] In future studies, we may use larger animal models to assess potential clinical application for human bone repair. As such animals have intact immune system, autologous MSCs will have to be used.

As shown in micro-CT results at 6 weeks, we did not observe robust bone formation in all groups, although the One step group showed the highest levels of BV and BMD compared to the other three groups (Figure 5). Since the thickness of skull bone of mouse

model is only several hundred microns, it is extremely difficult to hold the pre-fabricated gelatin scaffold within the defect area. Therefore, in this study, we needed first applied the hydrogel/cells/AAVs solution (before polymerization) to cover the defect area, and then used the VL to cure the gel in situ. By this way, the scaffolds were able to bind with the surrounding native bone tissues and stay in the position. However, the surface of the skull was not flat, the solution moved toward to the edge of defect. In order to have the gel cover the center area of defects, we had to make a relative thick hydrogel (around 1-2 mm). Because of the limited nutrition supply, cells inside the hydrogel either died, or did not generate sufficient matrix as those on the surface (Figure 7). However, we did observe the OCN-positive area the defect area in the One step or the Ex vivo groups, suggesting the osteogenesis on the surface area of scaffolds.

5 | CONCLUSION

We have developed an injectable, hBMSCs-loaded and gene-activated mGL hydrogel by means of VL-PXL for bone repair. The localized release of rAAV-BMP-2 constructs from the scaffold matrix was able to successfully transduce the encapsulated hBMSCs, resulting in the osteogenesis within the *BMP-2* gene-activated hydrogel. Results from the in vivo study showed promising applications of a one-step VL-PXL fabrication method for bone formation in local structural variation in different bone defects.

ACKNOWLEDGMENT

We thank the funding supports from U.S. Department of Defense (W81XWH-10-1-0850, W81XWH-14-2-0003) to Rocky S. Tuan. We acknowledge financial supports from the National Institutes of Health (5R01EB019430, to Rocky S. Tuan) and the Commonwealth of PA Department of Health (SAP4100061184 and SAP4100065563 to Bing Wang and Rocky S. Tuan; SAP4100050913 and SAP4100062224, to Rocky S. Tuan).

CONFLICT OF INTEREST

Rocky S. Tuan declare consultant/advisory role with Orthocell and research funding from Cerapedics. The other authors declared no potential conflicts of interest.

AUTHOR CONTRIBUTIONS

K.S., H.L.: equally involved in conception and design, collection and assembly of data, data analysis and interpretation, manuscript writing, final approval of manuscript; Y.T.: prepared the viral vectors and participated in the in vitro and in vivo study, and also contributed to micro-CT data; S.X.: analyzed the results of bone volume and bone mineral density; J.X., W.Y., J.T., H.P., P.G.A.: performed isolation of hBMSC, imaging, histology and immunohistochemistry and qPCR experiments, collection and assembly of data; R.S.T., B.W.: provided funding support, designed and supervised the study, and revised the manuscript. All authors read and approved the final manuscript.

DATA AVAILABILITY STATEMENT

The data that support the findings of this study are available on request from the corresponding author.

ORCID

Rocky S. Tuan https://orcid.org/0000-0001-6067-6705
Bing Wang https://orcid.org/0000-0002-5185-3500

REFERENCES

1. Peng H, Wright V, Usas A, et al. Synergistic enhancement of bone formation and healing by stem cel-expressed VEGF and bone morphogenetic protein-4. *J Clin Invest*. 2002;110(6):751-759.
2. Szpalski C, Barr J, Wetterau M, Saadeh PB, Warren SM. Cranial bone defects: current and future strategies. *Neurosurg Focus*. 2010;29(6):E8. https://doi.org/10.3171/2010.9.FOCUS10201.
3. Ewers R, Goriwoda W, Schopper C, Moser D, Spassova E. Histologic findings at augmented bone areas supplied with two different bone substitute materials combined with sinus floor lifting. Report of one case. *Clin Oral Implants Res*. 2004;15(1):96-100.
4. Shors EC. Coralline bone graft substitutes. *Orthop Clin North Am*. 1999;30(4):599-613.
5. Damien CJ, Parsons JR. Bone graft and bone graft substitutes: a review of current technology and applications. *J Appl Biomater*. 1991;2(3):187-208. https://doi.org/10.1002/jab.770020307.
6. Tuli R, Nandi S, Li WJ, et al. Human mesenchymal progenitor cell-based tissue engineering of a single-unit osteochondral construct. *Tissue Eng*. 2004;10(7–8):1169-1179. https://doi.org/10.1089/1076327041887628.
7. Stylios G, Wan T, Giannoudis P. Present status and future potential of enhancing bone healing using nanotechnology. *Injury*. 2007;38(Suppl 1):S63-S74. https://doi.org/10.1016/j.injury.2007.02.011.
8. Lee SH, Shin H. Matrices and scaffolds for delivery of bioactive molecules in bone and cartilage tissue engineering. *Adv Drug Deliv Rev*. 2007;59(4–5):339-359. https://doi.org/10.1016/j.addr.2007.03.016.
9. Mi MY, Tang Y, Salay MN, et al. AAV based ex vivo gene therapy in rabbit adipose-derived mesenchymal stem/progenitor cells for osteogenesis. *Open Stem Cell J*. 2009;1:69-75.
10. Lin H, Tang Y, Lozito TP, Oyster N, Wang B, Tuan RS. Efficient in vivo bone formation by BMP-2 engineered human mesenchymal stem cells encapsulated in a projection stereolithographically fabricated hydrogel scaffold. *Stem Cell Res Ther*. 2019;10(1):254. https://doi.org/10.1186/s13287-019-1350-6.
11. Lin H, Tang Y, Lozito TP, et al. Projection stereolithographic fabrication of BMP-2 gene-activated matrix for bone tissue engineering. *Sci Rep*. 2017;7(1):11327. https://doi.org/10.1038/s41598-017-11051-0.
12. Chen Y, Luk KD, Cheung KM, et al. Gene therapy for new bone formation using adeno-associated viral bone morphogenetic protein-2 vectors. *Gene Ther*. 2003;10(16):1345-1353. https://doi.org/10.1038/sj.gt.3301999.
13. Kumar S, Mahendra G, Nagy TR, Ponnazhagan S. Osteogenic differentiation of recombinant adeno-associated virus 2-transduced murine mesenchymal stem cells and development of an immunocompetent mouse model for ex vivo osteoporosis gene therapy. *Hum Gene Ther*. 2004;15(12):1197-1206.
14. Xue J, Lin H, Bean A, et al. One-step fabrication of bone morphogenetic protein-2 gene-activated porous poly-L-lactide scaffold for bone induction. *Mol Ther Methods Clin Dev*. 2017;7:50-59. https://doi.org/10.1016/j.omtm.2017.08.008.
15. Lin H, Cheng AW-M, Alexander PG, Beck AM, Tuan RS. Cartilage tissue engineering application of injectable gelatin hydrogel with in situ visible-light-activated gelation capability in both air and aqueous solution. *Tissue Eng Part A*. 2014;20(17–18):2402-2411.
16. Liu Y, Kuang B, Rothrauff BB, Tuan RS, Lin H. Robust bone regeneration through endochondral ossification of human mesenchymal stem

cells within their own extracellular matrix. *Biomaterials*. 2019;218:119336. https://doi.org/10.1016/j.biomaterials.2019.119336.
17. Yang Y, Lin H, Shen H, Wang B, Lei G, Tuan RS. Mesenchymal stem cell-derived extracellular matrix enhances chondrogenic phenotype of and cartilage formation by encapsulated chondrocytes in vitro and in vivo. *Acta Biomater*. 2018;69:71-82. https://doi.org/10.1016/j.actbio.2017.12.043.
18. Wang Z, Zhu T, Qiao C, et al. Adeno-associated virus serotype 8 efficiently delivers genes to muscle and heart. *Nat Biotechnol*. 2005;23(3):321-328. https://doi.org/10.1038/nbt1073.
19. Xiao X, Li J, Samulski RJ. Production of high-titer recombinant adeno-associated virus vectors in the absence of helper adenovirus. *J Virol*. 1998;72(3):2224-2232.
20. Wang B, Li J, Fu FH, et al. Construction and analysis of compact muscle-specific promoters for AAV vectors. *Gene Ther*. 2008;15(22):1489-1499. https://doi.org/10.1038/gt.2008.104.
21. Fairbanks BD, Schwartz MP, Bowman CN, Anseth KS. Photoinitiated polymerization of PEG-diacrylate with lithium phenyl-2,4,6-trimethylbenzoylphosphinate: polymerization rate and cytocompatibility. *Biomaterials*. 2009;30(35):6702-6707. https://doi.org/10.1016/j.biomaterials.2009.08.055.
22. Kim S, Tsao H, Kang Y, et al. In vitro evaluation of an injectable chitosan gel for sustained local delivery of BMP-2 for osteoblastic differentiation. *J Biomed Mater Res B Appl Biomater*. 2011;99(2):380-390. https://doi.org/10.1002/jbm.b.31909.
23. Wang B, Li J, Xiao X. Adeno-associated virus vector carrying human minidystrophin genes effectively ameliorates muscular dystrophy in mdx mouse model. *Proc Natl Acad Sci USA*. 2000;97(25):13714-13719. https://doi.org/10.1073/pnas.240335297.
24. Gao X, Usas A, Lu A, et al. BMP2 is superior to BMP4 for promoting human muscle-derived stem cell-mediated bone regeneration in a critical-sized calvarial defect model. *Cell Transplant*. 2013;22(12):2393-2408. https://doi.org/10.3727/096368912X658854.
25. Gao X, Usas A, Tang Y, et al. A comparison of bone regeneration with human mesenchymal stem cells and muscle-derived stem cells and the critical role of BMP. *Biomaterials*. 2014;35(25):6859-6870. https://doi.org/10.1016/j.biomaterials.2014.04.113.
26. Wang A, Ding X, Sheng S, Yao Z. Bone morphogenetic protein receptor in the osteogenic differentiation of rat bone marrow stromal cells. *Yonsei Med J*. 2010;51(5):740-745. https://doi.org/10.3349/ymj.2010.51.5.740.
27. Hoshiba T, Kawazoe N, Tateishi T, Chen G. Development of stepwise osteogenesis-mimicking matrices for the regulation of mesenchymal stem cell functions. *J Biol Chem*. 2009;284(45):31164-31173. https://doi.org/10.1074/jbc.M109.054676.
28. Asamura S, Mochizuki Y, Yamamoto M, Tabata Y, Isogai N. Bone regeneration using a bone morphogenetic protein-2 saturated slow-release gelatin hydrogel sheet: evaluation in a canine orbital floor fracture model. *Ann Plast Surg*. 2010;64(4):496-502. https://doi.org/10.1097/SAP.0b013e31819b6c52.
29. Lieberman JR, Daluiski A, Stevenson S, et al. The effect of regional gene therapy with bone morphogenetic protein-2-producing bone-marrow cells on the repair of segmental femoral defects in rats. *J Bone Joint Surg Am*. 1999;81(7):905-917.
30. D'Mello S, Atluri K, Geary SM, Hong L, Elangovan S, Salem AK. Bone regeneration using gene-activated matrices. *AAPS J*. 2017;19(1):43-53. https://doi.org/10.1208/s12248-016-9982-2.
31. Paul A, Manoharan V, Krafft D, et al. Nanoengineered biomimetic hydrogels for guiding human stem cell osteogenesis in three dimensional microenvironments. *J Mater Chem B*. 2016;4(20):3544-3554. https://doi.org/10.1039/C5TB02745D.
32. Gibbs DM, Black CR, Dawson JI, Oreffo RO. A review of hydrogel use in fracture healing and bone regeneration. *J Tissue Eng Regen Med*. 2016;10(3):187-198. https://doi.org/10.1002/term.1968.
33. Kidd ME, Shin S, Shea LD. Fibrin hydrogels for lentiviral gene delivery in vitro and in vivo. *J Control Release*. 2012;157(1):80-85. https://doi.org/10.1016/j.jconrel.2011.08.036.
34. Seidlits SK, Gower RM, Shepard JA, Shea LD. Hydrogels for lentiviral gene delivery. *Expert Opin Drug Deliv*. 2013;10(4):499-509. https://doi.org/10.1517/17425247.2013.764864.
35. Zhang H, Tang X, Wang C, Sun L. High-efficiency transduction of mesenchymal stem cells by Aav2/Dj vector for their potential use in autoimmune diseases. *Ann Rheum Dis*. 2018;77:1230. https://doi.org/10.1136/annrheumdis-2018-eular.5014.
36. Stender S, Murphy M, O'Brien T, et al. Adeno-associated viral vector transduction of human mesenchymal stem cells. *Eur Cell Mater*. 2007;13:93-99. discussion 9.
37. Alaee F, Sugiyama O, Virk MS, Tang Y, Wang B, Lieberman JR. In vitro evaluation of a double-stranded self-complementary adeno-associated virus type2 vector in bone marrow stromal cells for bone healing. *Genet Vaccines Ther*. 2011;9:4. https://doi.org/10.1186/1479-0556-9-4.
38. Rey-Rico A, Venkatesan JK, Frisch J, et al. PEO-PPO-PEO micelles as effective rAAV-mediated gene delivery systems to target human mesenchymal stem cells without altering their differentiation potency. *Acta Biomater*. 2015;27:42-52. https://doi.org/10.1016/j.actbio.2015.08.046.
39. Mah C, Fraites TJ Jr, Cresawn KO, Zolotukhin I, Lewis MA, Byrne BJ. A new method for recombinant adeno-associated virus vector delivery to murine diaphragm. *Mol Ther*. 2004;9(3):458-463. https://doi.org/10.1016/j.ymthe.2004.01.006.
40. Rey-Rico A, Venkatesan JK, Frisch J, et al. Effective and durable genetic modification of human mesenchymal stem cells via controlled release of rAAV vectors from self-assembling peptide hydrogels with a maintained differentiation potency. *Acta Biomater*. 2015;18:118-127. https://doi.org/10.1016/j.actbio.2015.02.013.
41. Schmidt C, Bezuidenhout D, Zilla P, Davies NH. A slow-release fibrin matrix increases adeno-associated virus transduction of wound repair cells in vivo. *J Biomater Appl*. 2014;28(9):1408-1418. https://doi.org/10.1177/0885328213510331.
42. McGovern JA, Griffin M, Hutmacher DW. Animal models for bone tissue engineering and modelling disease. *Dis Model Mech*. 2018;11(4). https://doi.org/10.1242/dmm.033084.
43. Gao X, Lu A, Tang Y, et al. Influences of donor and host age on human muscle-derived stem cell-mediated bone regeneration. *Stem Cell Res Ther*. 2018;9(1):316. https://doi.org/10.1186/s13287-018-1066-z.
44. Lee JC, Volpicelli EJ. Bioinspired collagen scaffolds in cranial bone regeneration: from bedside to bench. *Adv Healthc Mater*. 2017;6(17). https://doi.org/10.1002/adhm.201700232.

SUPPORTING INFORMATION

Additional supporting information may be found online in the Supporting Information section at the end of this article.

How to cite this article: Sun K, Lin H, Tang Y, et al. Injectable *BMP-2* gene-activated scaffold for the repair of cranial bone defect in mice. *STEM CELLS Transl Med*. 2020;9:1631–1642. https://doi.org/10.1002/sctm.19-0315